



TiO₂-Coated Carbon Nanotube-Silicon Solar Cells with Efficiency of 15%

SUBJECT AREAS:
CARBON NANOTUBES
AND FULLERENES
MATERIALS SCIENCE
MATERIALS FOR DEVICES
OPTICAL MATERIALS

Enzheng Shi¹, Luhui Zhang¹, Zhen Li², Peixu Li², Yuanyuan Shang¹, Yi Jia², Jinquan Wei², Kunlin Wang², Hongwei Zhu², Dehai Wu², Sen Zhang³ & Anyuan Cao¹

¹Department of Materials Science and Engineering, College of Engineering, Peking University, Beijing 100871, P. R. China, ²Key Laboratory for Advanced Materials Processing Technology and Department of Mechanical Engineering, Tsinghua University, Beijing 100084, P. R. China, ³Department of Energy and Resources Engineering, College of Engineering, Peking University, Beijing 100871, P. R. China.

Received
27 September 2012

Accepted
5 November 2012

Published
23 November 2012

Correspondence and
requests for materials
should be addressed to
A.C. (anyuan@pku.
edu.cn)

Combining carbon nanotubes (CNTs), graphene or conducting polymers with conventional silicon wafers leads to promising solar cell architectures with rapidly improved power conversion efficiency until recently. Here, we report CNT-Si junction solar cells with efficiencies reaching 15% by coating a TiO₂ antireflection layer and doping CNTs with oxidative chemicals, under air mass (AM 1.5) illumination at a calibrated intensity of 100 mW/cm² and an active device area of 15 mm². The TiO₂ layer significantly inhibits light reflectance from the Si surface, resulting in much enhanced short-circuit current (by 30%) and external quantum efficiency. Our method is simple, well-controlled, and very effective in boosting the performance of CNT-Si solar cells.

There have been intensive efforts in exploring innovated solar cell structures with high performance and cost-effective manufacturing methods^{1,2}. Emerging competitive technologies include solar cells based on organic molecules (with efficiencies of 7%)^{3,4}, colloidal quantum dots (efficiencies reaching 6%)^{5,6}, and dye-sensitized solar cells (efficiencies up to 12%)⁷⁻⁹. An alternative approach is to combine inexpensive materials with well-established semiconductors (e.g. silicon) to create new architectures that have the potential of simplifying fabrication processes and lowering cost. To this end, researchers have explored various candidates, particularly transparent conductive films of carbon nanotubes (CNTs), graphene and semiconducting polymers that can be conveniently deposited on commercial Si wafers to make efficient solar cells¹⁰⁻¹⁸. During the past years, considerable progresses have been achieved in this area and power conversion efficiencies have been steadily enhanced to about 8% for graphene-Si¹⁷ and 13.8% for acid-doped CNT-Si cells¹³. At this high level, even 1% increase of efficiency is critical for pushing forward practical applications and sometimes requires substantial modification or improvement of current cell structures.

The light-to-electricity conversion in a solar cell involves several key steps, including light absorption, charge separation and carrier collection. The light absorption step determines how much fraction of incident photons can be absorbed by the semiconductor and the excitation of charge carriers, therefore directly influences the external quantum efficiency and cell efficiency. For planar substrates such as polished Si, light reflection from their surface could be as high as 36%, resulting in substantial energy loss in the light absorption stage¹⁹. Antireflection structures such as vertical semiconducting nanowire arrays grown on or etched from a Si substrate²⁰, nanodome-like amorphous Si films²¹, and patterned Si nanocones¹⁸ with suitable aspect ratios have been reported recently, and showed effective light trapping and reflection reduction for the devices. Those approaches generally created a rough surface on top of the Si substrate and involved complex photolithography techniques to make patterns. In addition, the non-smooth Si surface may prevent conformal transfer of nanotube or graphene films and bring additional charge recombination sites, for example, on the surface of patterned nanowires and nanocones.

Recently, several groups and our team have particularly studied CNT-silicon solar cells that were fabricated by transferring a semi-transparent CNT film onto a n-type single-crystalline Si wafer to form Schottky junctions and heterojunctions^{10-15,22}. By applying a series of doping and gating methods such as SOCl₂ treatment²², ionic liquid electrolyte infiltration and electronic gating^{14,15} as well as nitric acid doping¹³, the power conversion efficiencies of these CNT-Si cells have been continuously pushed from initially about 1.3% to 13.8% (a ten-fold increase) during the past several years, indicating a very promising architecture with reduced manufacturing cost and also the potential of achieving high performance.



Here, we report an improved device structure, a TiO₂-coated CNT-Si (TiO₂-CNT-Si) solar cell, with measured power conversion efficiencies reaching above 15% under air mass (AM 1.5) global illumination conditions after chemical doping. The main original idea is to introduce a TiO₂ colloidal antireflection layer on the top to boost the cell efficiency to a higher level. The spin-coating process was very simple and layer thickness well controlled. Mechanism study revealed that the TiO₂ coating reduced light reflection from the cell surface to less than 10%, enhanced the short-circuit current by 30% and external quantum efficiency to nearly 90% in the visible region.

Results

Our fabrication of TiO₂-CNT-Si solar cells involved the following steps, as illustrated in Fig. 1 (see Experimental for details). The single-walled nanotube films were synthesized by chemical vapor deposition (CVD) with controlled optical transparency and sheet resistance, as described in our previous reports²³. We started from a *n*-type Si wafer with 400 nm oxide, and transferred a CNT film onto the oxide surface to form smooth contact. Micrometer-thick Ag paste was applied around to enclose a nearly square-shaped window and define the active device area (about 15 mm²). The surrounding Ag paste was thick enough to prevent light penetration to the underlying Si from outside of the window, thus ensure precise calculation of the current density (output current divided by device area). Inside the window, the SiO₂ was removed by HF vapor etching, resulting in direct CNT-Si contact and junction formation. After that, a TiO₂ nanoparticle colloid synthesized by sol-gel method²⁴ was spin-coated at an appropriate thickness (50–80 nm) onto the CNT film. Characterization of the TiO₂ colloid and solid layer by transmission electron microscopy (TEM), UV-Visible absorption and Raman spectrum revealed aggregations of crystalline nanoparticles with diameters of several nanometers and an absorption range at 350 nm (corresponding to a bandgap of ~4 eV) (Supplementary Information, Fig. S1). Before solar cell measurements, the device was sequentially exposed to nitric acid and hydrogen peroxide vapors for a few seconds for doping CNTs. Here, the TiO₂ coating and chemical doping are two critical steps in order to obtain maximum efficiency, in which the TiO₂ layer mainly increases the current density and the latter improves fill factor (discussed later).

We have characterized the morphology of CNT-Si cells and the TiO₂ layer by optical and scanning electron microscope (SEM). Our typical device area (~15 mm²) allows spin-coating of a uniform TiO₂ layer on top of the CNT film. Before coating, the CNT-Si cell

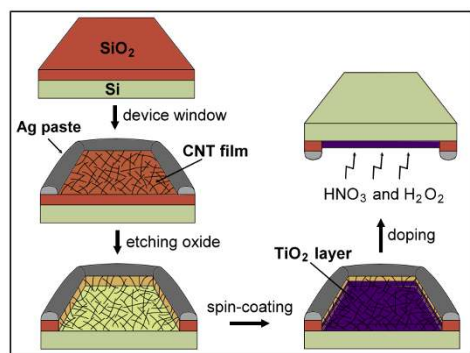


Figure 1 | Illustration of the fabrication process of a TiO₂-CNT-Si solar cell involving the following steps: 1) creating a cell device window by transferring a CNT film on a Si wafer (with 400 nm oxide) and applying Ag paste around the film, 2) etching away the oxide layer to form direct CNT-Si contact and junction, 3) spin-coating a thin TiO₂ colloid on top of the CNT film as antireflection layer, and 4) chemical doping of the cell by vapor of HNO₃ and H₂O₂.

surface appears to be bright because the CNT film is so thin and the planar Si substrate is reflective (Fig. 2a). In contrast, the cell coated by TiO₂ shows a dark blue-to-violet color, indicating effective reduction of light reflection (Fig. 2b). SEM image of the bare cell shows the spiderweb-like CNT film consisting of interconnected nanotube bundles with diameters of several to tens of nanometers. After spin-coating, the nanotube features can not be distinguished easily. Instead, we observe a uniform film of aggregated TiO₂ nanoparticles. The TiO₂ colloid covers not only the top of every nanotube bundle but also the porous area among the CNT network, therefore could form good adhesion to the Si substrate and ensure uniform thickness across the CNT film (Fig. 2c, 2d). Before and after HNO₃/H₂O₂ doping, the TiO₂ layer shows similar morphology by SEM characterization (Fig. S2), indicating that the chemical vapors could penetrate through the layer to affect the underlying device. Cross-sectional view obtained by breaking the cell at the middle reveals the layer thickness of about 70 nm (ranging from 50 to 80 nm for different samples with slight fluctuation), and the CNTs are embedded within the bottom part of TiO₂ layer yet still maintain contact to Si (Fig. 2e, 2f). Many CNT bundles hang down on the fractured cross-section of Si wafer, indicating good strength and interconnection. There are also some tiny (nanoscale) protrusions present on the TiO₂ layer, which could help light trapping like nanocones. The TiO₂ layer thickness is controlled by the rotation speed during spin-coating, and most of areas in the middle of the solar cell have uniform thickness except for the edge portion where the layer meets Ag paste resulting in increased thickness (Fig. S3).

We have measured the current density-voltage (*J*-*V*) characteristics in the dark and light conditions under AM 1.5 at calibrated intensities of 70 to 100 mW/cm². The TiO₂-CNT-Si cell shows a short-circuit current density (*J*_{sc}) of 32 mA/cm², an open-circuit voltage (*V*_{oc}) of 0.61 V, a fill factor (*FF*) of 77%, resulting in an efficiency of 15.1% at 100 mW/cm² (Fig. 3a). The *J*_{sc} decreases

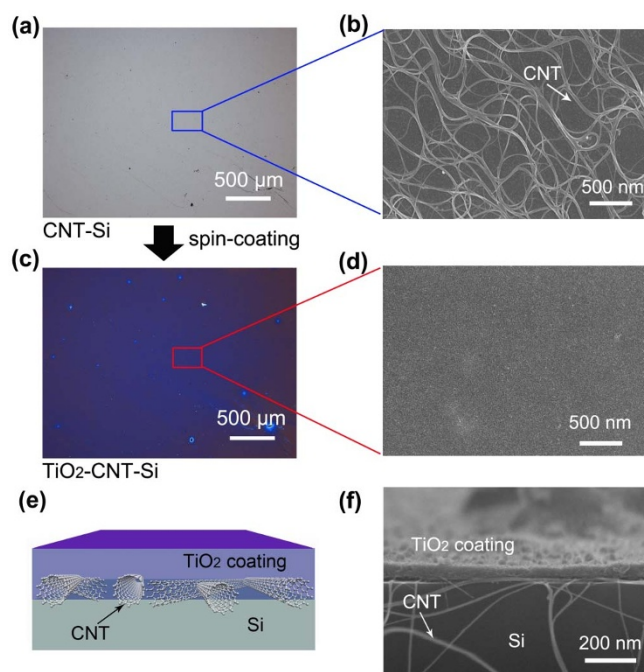


Figure 2 | Characterization of TiO₂-CNT-Si solar cells. (a) Optical image of a CNT-Si cell without coating. (b) SEM image of the CNT film transferred to the Si wafer. (c) Optical image of this cell after spin-coating a TiO₂ layer, showing color change of appearance. (d) SEM image on the cell surface showing a uniform layer of TiO₂ covered on top of the CNTs. (e) Illustrated solar cell structure consisting of a Si substrate, a CNT film and a TiO₂ layer. (f) Cross-sectional SEM image of the cell after coating.



consistently under reduced illumination intensity, and the cell efficiency is 15.3% for an intensity of 90 mW/cm², about 14.8% for 80 and 70 mW/cm². The high efficiency (15%) is attributed to a combination of good parameters including very high *FF* (77%) and reasonable *J_{sc}* and *V_{oc}* values. Previously, there were several relevant Si-based hybrid cells using different strategies to obtain good performance. Among those, patterned CNT grid lines filled with ionic electrolyte at a gate voltage (−0.75 V) showed a comparable *J_{sc}* (29.8 mA/cm²) and efficiency of 12%¹⁵. A CNT-Si cell with nitric acid infiltration into the CNT network showed higher *J_{sc}* (36.3 mA/cm²) but lower *V_{oc}* (0.53 V) and *FF* (72%), with an efficiency of 13.8%¹³. A conjugated polymer-Si nanocone cell (antireflection structure) with top Au grid had a similar *J_{sc}* (31 mA/cm²) but lower *V_{oc}* (0.50 V) and *FF* (63%), with an efficiency of 11%¹⁸. Compared with those structures, our TiO₂-CNT-Si cells are free from liquids and do not use metal contacts on top of the active junction area.

We found that the TiO₂ coating and subsequent chemical doping are responsible for improving the current density and fill factor, respectively. To study these effects, *J*-*V* curves of solar cells after each step were recorded and plotted together (Fig. 3b). An original bare CNT-Si cell without treatments had an efficiency of about 8%, and after coating TiO₂, the *J_{sc}* increased from 24.4 to 32.2 mA/cm². The enhancement of *J_{sc}* by more than 30% indicates that the TiO₂ layer is very effective in increasing the current density (due to antireflection). However, it does not influence the values of *V_{oc}* and *FF*. The second step was done by exposing the TiO₂-CNT-Si cell to H₂O₂ and HNO₃ vapors sequentially for 5 to 15 seconds, which caused the *FF* to increase from 65% to 74% while the *J_{sc}* remained unchanged. The combined effects yielded much enhanced cell efficiency of 14.5%. For

the three parameters that determine the final cell efficiency, *J_{sc}*, *V_{oc}* and *FF*, TiO₂ mainly improves *J_{sc}* while exposure to H₂O₂/HNO₃ mainly improves *FF*. Our previous work has demonstrated that HNO₃ doping can improve solar cell efficiency by reducing the sheet resistance of CNT films and possibly forming oxide on Si surface¹². Here, we found that the maximum *FF* was obtained by combining HNO₃ with H₂O₂ vapor treatments, likely because that oxygen bubbles generated from H₂O₂ could produce tiny pores or cracks in the TiO₂ layer similar to previous reports on TiO₂ and other oxides^{25,26}, making it easier for HNO₃ vapor to penetrate through TiO₂ and reach the CNT film.

The effect of TiO₂ coating can also be seen from the incident photon to current efficiency (IPCE) results, a measurement of external quantum efficiency (EQE) (Fig. 3c). The same original CNT-Si cell as in Fig. 3b showed a flat IPCE of about 60% from 400 to 1000 nm corresponding to the wavelength absorption range of Si (1.12 eV), indicating that the Si substrate is responsible for photon absorption and carrier generation. After coating TiO₂, there was a pronounced increase of IPCE in the same region, which reached nearly 90% from 600 to 800 nm. The current density values calculated from the accumulating area under each curve were 23.8 and 31.7 mA/cm² before and after coating, respectively, very close to the *J_{sc}* values in the *J*-*V* curves in Fig. 3b (24.4 and 32.2 mA/cm²). In comparison, the EQE of the graphene-Si model with cell efficiency of 8.6% was between 60% to 70%¹⁷, similar to our un-coated cell with efficiency of 8.25% and IPCE of 60%. Another work on polymer-Si nanocone cells reported an EQE of 70% to 90% (with or without top Au grid) and cell efficiency of 11% owing to the antireflection device structure¹⁸. Therefore the process of TiO₂ coating could improve

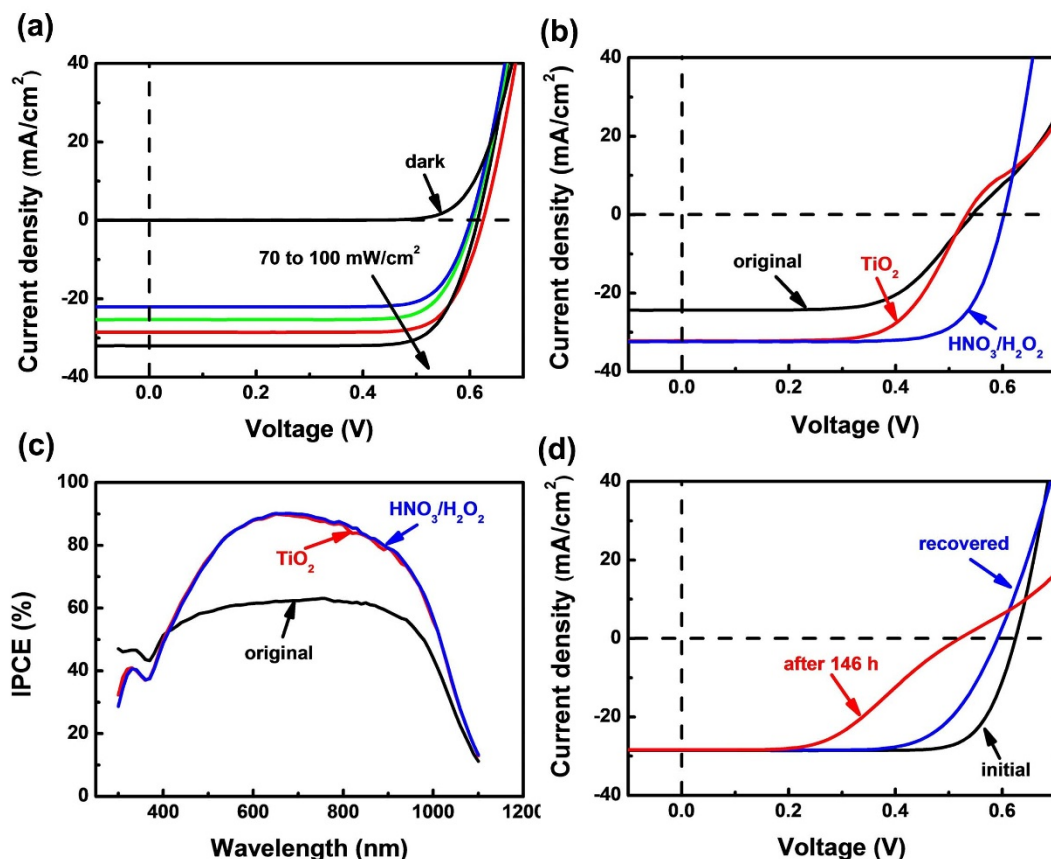


Figure 3 | Solar cell characteristics. (a) *J*-*V* curves of a TiO₂-CNT-Si cell measured in the dark and light conditions (from 70 to 100 mW/cm²). (b) *J*-*V* curves of a CNT-Si cell recorded in original state (without coating), with a TiO₂ antireflection layer, and after HNO₃/H₂O₂ treatment, respectively. (c) IPCE data of the same cell in original state, with a TiO₂ layer, and after doping, respectively. (d) *J*-*V* curves of a TiO₂-CNT-Si cell measured in initial state (maximum efficiency), after storing 146 hours in air without encapsulation, and recovered by chemical doping again (light intensity: 90 mW/cm²).



IPCE significantly, which was directly related to the 30% increase of J_{sc} observed in J - V curves (Fig. 3b). Another consistent result was that the $\text{HNO}_3/\text{H}_2\text{O}_2$ treatment did not increase IPCE at all (Fig. 3c), and in the corresponding J - V curves we can see that only FF was affected by such chemical doping while J_{sc} remained constant (Fig. 3b).

Since our process involved chemical doping, it is necessary to investigate the device stability during storage. We found that the effect of $\text{HNO}_3/\text{H}_2\text{O}_2$ treatment could last for several hours, in which the FF maintained a high value (larger than 70%). For long time storage in air without using additional encapsulation techniques, the FF dropped from 77% to 48.5% after 146 hours exposure to air although the J_{sc} remained unchanged (Fig. 3d). However, a $\text{HNO}_3/\text{H}_2\text{O}_2$ treatment again could recover the FF to 68.6% immediately and the J - V curve also shifted toward the original state. Certainly, the stability issues caused by chemical doping need be addressed in the future, for example, by selecting more stable doping agents. Here, one of the advantages in our cells is that the TiO_2 coating not only serves as the antireflection layer, but also protects the underlying CNT-Si junction and ensures a stable J_{sc} over long time (previously TiO_2 film was deposited onto organic solar cells to improve stability²⁷).

Discussion

The main effect of the TiO_2 layer in our solar cells was antireflection, as proved by light reflection measurements and other control experiments. Without coating, a bare CNT-Si cell showed a reflectance of 30% to 40%. With a 70 nm TiO_2 layer, the light reflectance dropped substantially in the visible region, especially to a minimum value (<5%) at around 600 nm (Fig. 4a). The overall reflectance was inhibited to less than 10% to 20% across the spectrum. Recall that the maximum IPCE (nearly 90%) of a TiO_2 -coated cell also occurred at

the position of 600 to 800 nm (Fig. 3c). If we assume a refractive index of 1 for air, the condition for a coating to generate destructive interference at the air-coating interface can be expressed by $d_{\text{TiO}_2} = \frac{\lambda}{4n_{\text{TiO}_2}}$, where λ is incident light wavelength, d_{TiO_2} is the layer thickness and n_{TiO_2} is the refractive index for TiO_2 nanoparticles (~ 2.2)¹⁹ (as illustrated in Fig. 4b). Given an incident wavelength of $\lambda = 600$ nm (where maximum antireflection occurs), the calculated optimal layer thickness is 68 nm which is well within the thickness range of our spin-coated TiO_2 layers (50–80 nm). While other structures such as periodic nanodome and nanocone arrays can re-direct the route of light transport for light scattering and trapping, here we used a thin TiO_2 layer to serve as an interference antireflection coating.

Because TiO_2 nanoparticles were directly deposited on CNTs, electronic interaction might exist between TiO_2 and CNTs as revealed in some semiconducting nanoparticle-CNT hybrid systems²⁸. To study this, a CNT film was put on an insulating silica sheet and TiO_2 colloid was spin-coated on top of CNTs. We configured a two-probe device by contacting the two sides of the TiO_2 -covered CNT film and scanning the voltage from -1 to 1 V (inset of Fig. 4c). If electron transfer from the TiO_2 nanoparticles to CNTs occurs under light excitation, the current flow through the device should change accordingly. However, under illumination ($90 \text{ mW}/\text{cm}^2$) the current-voltage curve almost did not change (Fig. 4c). Combining with the IPCE results where no peaks corresponding to the TiO_2 bandgap appear, we think that the TiO_2 coating only serves as the antireflection layer and does not provide appreciable charge carriers for the solar cell.

Finally, we studied the effect of TiO_2 layer thickness on solar cell characteristics. With increasing layer thickness from about 60 to

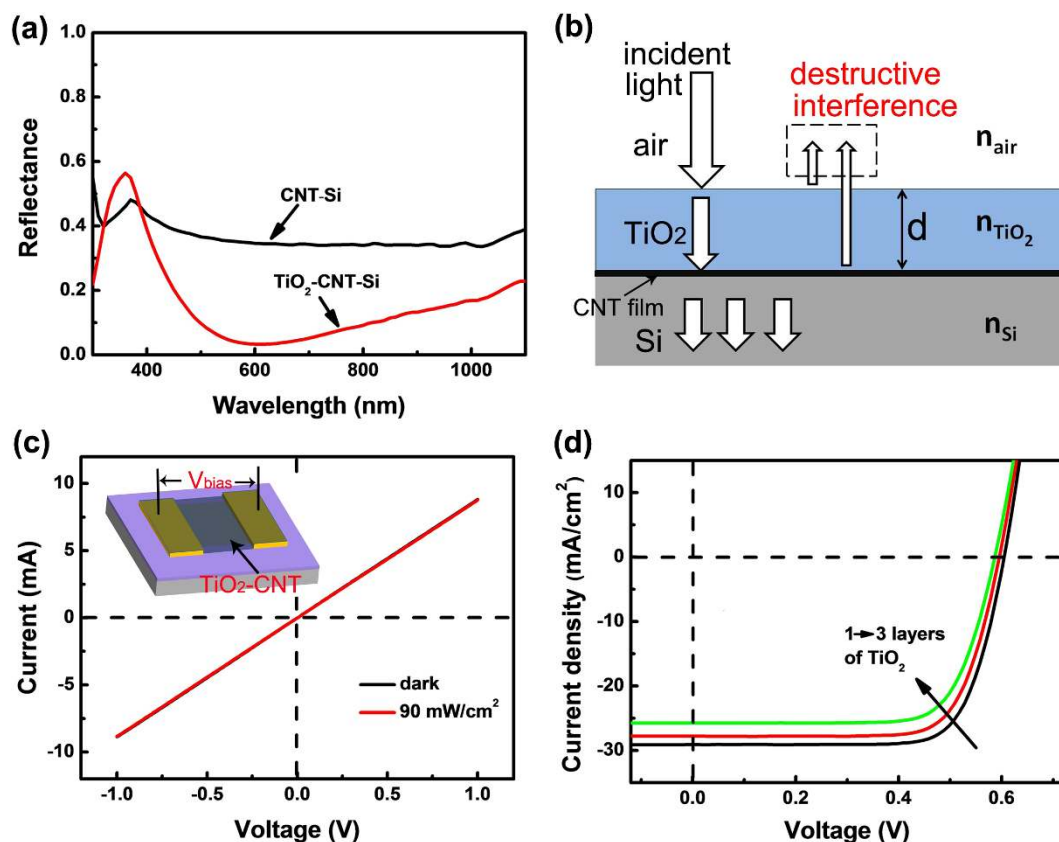


Figure 4 | Mechanism study. (a) Light reflectance of a CNT-Si cell before and after TiO_2 coating. (b) Illustration of the reflection reduction effect by the TiO_2 layer. Destructive interference occurs at the layer surface when the layer thickness (d) is appropriate. (c) Current-voltage curves of a TiO_2 -coated CNT film under a bias of 1 V in the dark and light ($90 \text{ mW}/\text{cm}^2$), respectively. Inset shows the device setup (on an insulating substrate). (d) J - V curves of a CNT-Si cell with 1 to 3 coated TiO_2 layers (thickness from 60 to 180 nm) under $90 \text{ mW}/\text{cm}^2$.



180 nm, the current densities produced under the same illumination intensity dropped slightly from 29.1 to 25.8 mA/cm² and the cell efficiency decreased from 14.6% to 12.3% (Fig. 4d). There are two factors underlying this phenomenon. First, an optimum layer thickness of about 60–80 nm exists in our solar cells for maximum inhibition of light reflection in the visible range, determined by the 1/4 wavelength relationship (Fig. 4b). Second, although TiO₂ is almost transparent to visible light, a thick layer consisting of aggregated nanoparticles may produce light scattering and reduce incident light to Si. A previous report has used a slightly thinner TiO₂ layer (48 nm in thickness) to reduce light reflection in p-n junction Si solar cells¹⁹.

In conclusion, a CNT-Si solar cell with efficiency of 15% was reported. Our results indicate one step further for constructing alternative high performance Si-based photovoltaics with advantages in cost reduction and process simplification. This efficiency is also important for practical applications and commercialization of this type of solar cells in the future. The TiO₂ antireflection layer represents an effective strategy to improve the efficiency of CNT-Si solar cells and possibly other similar models such as the graphene-Si structures.

Methods

Synthesis of CNT films and TiO₂ nanoparticles. Single-walled CNT films were grown by CVD using a source solution of ferrocene (0.045 g/mL) and sulfur (0.001 g/mL) dissolved in xylene. The solution was injected into the upstream side (200–250 °C) at rates of 3–5 μL/min by a syringe pump, and the vapor was carried to the reaction zone by a mixture of argon and hydrogen (volume ratio of Ar/H₂ is equal to 0.85:0.15) flowing at 1500 standard cubic centimeters per minute (sccm). Growth temperature was set at 1160 °C and typical reaction time was 30 minutes. Spiderweb-like CNT films were floating to the downstream end and collected by substrates. For synthesis of TiO₂ colloid, about 5 mL Ti(OBu)₄, 23 mL ethanol and 0.5 mL ethyl acetate were mixed in a flask as precursors. Then a hydrolysate solution containing 1.5 mL HNO₃ (0.1 mol/L), 1.5 mL de-ionized water and 12 mL ethanol was added by droplets into the precursor solution at a rate of 0.5–1 mL/min. The mixture was stirred continuously for 12 hours at 800 rpm (revolutions per minute) and then aged for 12 hours at room temperature.

Fabrication of TiO₂-CNT-Si solar cells. Commercially available n-type, 4-inch diameter, 400 μm-thick Si wafers with 400 nm-thick oxide and bulk resistivities of 0.05–0.2 Ω·cm were cut into pieces and used as substrates. As-synthesized CNT films were immersed in H₂O₂ and HCl to remove amorphous carbon and wash away residue catalyst. A purified expanded film was transferred onto the surface of Si (oxide) to make a conformal contact. At the front, micrometer-thick Ag paste was applied around the film to enclose a nearly square window as the device area. Back contact was made by applying liquid-state gallium-indium eutectic (E-GaIn) onto the back side of Si wafer. The SiO₂ inside the window was removed by exposing the device (CNT side) to HF vapor for 2–3 minutes resulting in direct CNT-Si contact. The device was placed in ethanol vapor for a few hours to clean the surface. After that, a TiO₂ nanoparticle colloid was spin-coated onto the device surface at 5000–6000 rpm for 1 minute, making a uniform antireflection layer with a thickness of 50–80 nm. The spin-coating process was repeated at the same parameters for coating multiple TiO₂ layers. Chemical doping was done by placing the cell downward on the vapor of concentrated HNO₃ and H₂O₂ (30% in water) sequentially for 15 seconds each.

Characterization and electrical measurements. The structure and morphology of CNT films, TiO₂ layer and solar cells were characterized by optical microscope (Olympus BX51M), Raman Spectrometer (Renishaw inVia plus), SEM (Hitachi S4800) and TEM (FEI Tecnai G2 T20). Solar cell characteristics were tested by a source meter (Keithley 2635A) and a solar simulator (Newport Thermo Oriol 91195A-1000) under AM 1.5G condition at an illumination intensity of 70–100 mW/cm², calibrated by a standard Si solar cell (91150V). IPCE and optical reflectance were measured by solar cell QE/IPCE measurement system (Zolix solar cell scan100) across a wavelength range of 300–1100 nm.

- Lewis, N. S. Toward cost-effective solar energy use. *Science* **315**, 798–801 (2007).
- Grätzel, M. Photoelectrochemical cells. *Nature* **414**, 338–344 (2001).
- Liang, Y. Y. *et al.* For the bright future-bulk heterojunction polymer solar cells with power conversion efficiency of 7.4%. *Adv. Mater.* **22**, E135–E138 (2010).
- Sun, Y. M. *et al.* Solution-processed small-molecule solar cells with 6.7% efficiency. *Nature Mater.* **11**, 44–48 (2012).
- Pattantyus-Abraham, A. G. *et al.* Depleted-heterojunction colloidal quantum dot solar cells. *ACS Nano* **4**, 3374–3380 (2010).

- Tang, J. *et al.* Colloidal-quantum-dot photovoltaics using atomic-ligand passivation. *Nature Mater.* **10**, 765–771 (2011).
- Han, L. Y. *et al.* High-efficiency dye-sensitized solar cell with a novel co-adsorbent. *Energy Environ. Sci.* **5**, 6057–6060 (2012).
- Yella, A. *et al.* Porphyrin-sensitized solar cells with cobalt (II/III)-based redox electrolyte exceed 12 percent efficiency. *Science* **334**, 629–634 (2011).
- Chung, I., Lee, B., He, J. Q., Chang, R. P. H. & Kanatzidis, M. G. All-solid-state dye-sensitized solar cells with high efficiency. *Nature* **485**, 486–490 (2012).
- Wei, J. Q. *et al.* Double-walled carbon nanotube solar cells. *Nano Lett.* **7**, 2317–2321 (2007).
- Jia, Y. *et al.* Nanotube-silicon heterojunction solar cells. *Adv. Mater.* **20**, 4594–4598 (2008).
- Jia, Y. *et al.* Encapsulated carbon nanotube-oxide-silicon solar cells with stable 10% efficiency. *Appl. Phys. Lett.* **98**, 133115 (2011).
- Jia, Y. *et al.* Achieving high efficiency silicon-carbon nanotube heterojunction solar cells by acid doping. *Nano Lett.* **11**, 1901–1905 (2011).
- Wadhwa, P., Liu, B., McCarthy, M. A., Wu, Z. C. & Rinzler, A. G. Electronic junction control in a nanotube-semiconductor Schottky junction solar cell. *Nano Lett.* **10**, 5001–5005 (2010).
- P. Wadhwa, P., Seol, G., Petterson, M. K., Guo, J. & Rinzler, A. G. Electrolyte-induced inversion layer Schottky junction solar cells. *Nano Lett.* **11**, 2419–2423 (2011).
- Tune, D. D., Flavel, B. S., Krupke, R. & Shapter, J. G. Carbon nanotube-silicon solar cells. *Adv. Energy Mater.* **2**, 1043–1055 (2012).
- Miao, X. *et al.* High efficiency graphene solar cells by chemical doping. *Nano Lett.* **12**, 2745–2750 (2012).
- Jeong, S. *et al.* Hybrid silicon nanocone-polymer solar cells. *Nano Lett.* **12**, 2971–2976 (2012).
- Pettit, R. B., Brinker, C. J. & Ashley, C. S. Sol-gel double-layer antireflection coatings for silicon solar cells. *Solar Cells* **15**, 267–278 (1985).
- Garnett, E. & Yang, P. D. Light trapping in silicon nanowire solar cells. *Nano Lett.* **10**, 1082–1087 (2010).
- Zhu, J., Hsu, C.-M., Yu, Z. F., Fan, S. H. & Cui, Y. Nanodome solar cells with efficient light management and self-cleaning. *Nano Lett.* **10**, 1979–1984 (2010).
- Li, Z. R. SOCl₂ enhanced photovoltaic conversion of single wall carbon nanotube/n-silicon heterojunctions. *Appl. Phys. Lett.* **93**, 243117 (2008).
- Li, Z. *et al.* Large area, highly transparent carbon nanotube spiderwebs for energy harvesting. *J. Mater. Chem.* **20**, 7236–7240 (2010).
- Han, H. & Bai, R. B. Buoyant photocatalyst with greatly enhanced visible-light activity prepared through a low temperature hydrothermal method. *Ind. Eng. Chem. Res.* **48**, 2891–2898 (2009).
- Arabatzis, I. M. & Falaras, P. Synthesis of porous nanocrystalline TiO₂ foam. *Nano Lett.* **3**, 249–251 (2003).
- Chandrupa, G. T., Steunou, N. & Livage, J. Macroporous crystalline vanadium oxide foam. *Nature* **416**, 702 (2002).
- Lee, K. *et al.* Air-stable polymer electronic devices. *Adv. Mater.* **19**, 2445–2449 (2007).
- Li, X. L., Jia, Y. & Cao, A. Y. Tailored single-walled carbon nanotube-CdS nanoparticle hybrids for tunable optoelectronic devices. *ACS Nano* **4**, 506–512 (2010).

Acknowledgments

This work was supported by the National Science Foundation of China (NSFC) under the grant number of 51072005.

Author contributions

E.S. designed experiments and performed solar cell fabrication, characterization and tests. L.Z., Z.L. and Y.S. synthesized TiO₂ colloids and CNT films. P.L. and Y.J. participated in device fabrication and optimization. S.Z. performed optical reflection measurements. D.W. and A.C. designed experiments. E.S. and A.C. wrote the paper. All authors contributed to discussion, analysis of results and preparation of manuscript.

Additional information

Supplementary information accompanies this paper at <http://www.nature.com/scientificreports>

Competing financial interests: The authors declare no competing financial interests.

License: This work is licensed under a Creative Commons Attribution-NonCommercial-NoDerivs 3.0 Unported License. To view a copy of this license, visit <http://creativecommons.org/licenses/by-nc-nd/3.0/>

How to cite this article: Shi, E. *et al.* TiO₂-Coated Carbon Nanotube-Silicon Solar Cells with Efficiency of 15%. *Sci. Rep.* **2**, 884; DOI:10.1038/srep00884 (2012).